International Geology Review
Publication details, including instructions for authors and subscription information:
http://www.tandfonline.com/loi/tigr20

Zircon U-Pb age and Sr-Nd-Hf isotopic constraints on the age and origin of Triassic mafic dikes, Dalian area, Northeast China

Shen Liu [a], Ruizhong Hu [a], Shan Gao [b], Caixia Feng [a], Ian M. Coulson [c], Guangying Feng [a], Youqiang Qi [a], Yuhong Yang [a], Chaogui Yang [a] & Liang Tang [a]

[a] State Key Laboratory of Ore Deposit Geochemistry, Institute of Geochemistry, Chinese Academy of Sciences, Guiyang, 550002, China

[b] State Key Laboratory of Geological Processes and Mineral Resources, China University of Geosciences, Wuhan, 430074, China

[c] Solid Earth Studies Laboratory, Department of Geology, University of Regina, Regina, SK, Canada, S4S 0A2

Published online: 17 Jul 2012.

To cite this article: Shen Liu, Ruizhong Hu, Shan Gao, Caixia Feng, Ian M. Coulson, Guangying Feng, Youqiang Qi, Yuhong Yang, Chaogui Yang & Liang Tang (2013) Zircon U-Pb age and Sr-Nd-Hf isotopic constraints on the age and origin of Triassic mafic dikes, Dalian area, Northeast China, International Geology Review, 55:2, 249-262, DOI: 10.1080/00206814.2012.707003

To link to this article: http://dx.doi.org/10.1080/00206814.2012.707003

International Geology Review
Vol. 55, No. 2, 20 January 2013, 249–262

Zircon U–Pb age and Sr–Nd–Hf isotopic constraints on the age and origin of Triassic mafic dikes, Dalian area, Northeast China

Shen Liu[a]*, Ruizhong Hu[a], Shan Gao[b], Caixia Feng[a], Ian M. Coulson[c], Guangying Feng[a], Youqiang Qi[a], Yuhong Yang[a], Chaogui Yang[a] and Liang Tang[a]

[a]*State Key Laboratory of Ore Deposit Geochemistry, Institute of Geochemistry, Chinese Academy of Sciences, Guiyang 550002, China;* [b]*State Key Laboratory of Geological Processes and Mineral Resources, China University of Geosciences, Wuhan 430074, China;* [c]*Solid Earth Studies Laboratory, Department of Geology, University of Regina, Regina, SK, Canada S4S 0A2*

(*Accepted 23 June 2012*)

Post-orogenic mafic rocks from Northeast China consist of swarms of dolerite dikes. We report a new U–Pb zircon age, as well as whole-rock geochemical and Sr–Nd–Hf isotopic data. Laser ablation inductively coupled plasma mass spectrometry (LA–ICP–MS) U–Pb zircon analysis yielded an age of 210.3 ± 1.5 million years (i.e. Triassic) for these mafic dikes. Most Dalian mafic rocks exhibit low $K_2O + Na_2O$ contents, and span the border between alkaline and calc-alkaline rock associations in the total alkali–silica diagram. The investigated dikes are also characterized by relatively high $(^{87}Sr/^{86}Sr)_i$ ratios (0.7061–0.7067) and negative $\varepsilon_{Nd}(t)$ (−4.7 to −4.3) and $\varepsilon_{Hf}(t)$ values (−4.1 to −1.1), implying that they were derived from an enriched lithospheric mantle source. The mafic dikes are characterized by relatively low MgO (4.65–5.44 wt.%), $Mg^{\#}$ (41–44), and compatible element content [such as Cr (89.9–125 ppm) and Ni (56.7–72.2 ppm)], which are the features of an evolved mafic magma. No evidence supports the idea that the mafic rocks were affected by significant assimilation or crustal contamination during emplacement. We conclude that the dolerites formed in a post-orogenic extensional setting, related to lithospheric delamination or 'collapse' of the Central Asian Orogenic Belt (CAOB), also termed the Xingmeng Orogenic Belt in China.

Keywords: post-orogenic; Triassic magmatism; mafic dikes; lithospheric delamination; crustal extension; Northeast China

1. Introduction

Mesozoic mafic dikes are widespread in Northeast China. These dolerites formed as a result of important extension of the continental lithosphere (Hall 1982; Hall and Fahrig 1987; Tarney and Weaver 1987; Zhao and McCulloch 1993). Studies of these rift-related dikes are essential for an enhanced understanding of the generation of such widespread episodes of mafic magmatism, providing valuable information concerning the Mesozoic lithospheric evolution beneath the North China Craton (NCC) (Liu *et al*. 2004, 2006, 2008a, 2008b, 2009, 2010b, 2010c) in this part of East Asia.

Despite a number of investigations of mafic dikes present in east Jilin and Heilongjiang provinces, controversy remains concerning their origins and significance (e.g. Qin 1995; Wu *et al*. 2004; Zhu *et al*. 2009; Liu *et al*. 2010b). Moreover, while a few investigations of Mesozoic mafic dikes in the eastern NCC (i.e. Liaoning Province) have been reported (Yang *et al*. 2004; Pei *et al*. 2005; Song and Qiao 2008; Liu *et al*. 2010a; Feng *et al*. 2011), to date there are no studies of Mesozoic mafic dikes present in the vicinity of Dalian.

Accordingly, our study provides an excellent opportunity to further document the ages and chemical and isotopic characteristics of Mesozoic mafic dike swarms in Northeast China; herein, we present a systematic isotopic and geochemical investigation of representative mafic dolerite dikes from Dalian. In addition, we report new ages and Sr–Nd–Hf isotopic data to help constrain their petrogenesis. These data are then used to discuss the Mesozoic evolution of the mantle sources that provided these NCC mafic magmas.

2. Geological setting and petrology

The Nenjiang and Mudanjiang faults divide Northeast China into three contrasting microcontinental blocks: the Jiamusi Block in the east, the Songliao Block in the central part, and the Xing'an Block in the northwest (Ye *et al*. 1994; Wu *et al*. 1995). The Jiamusi Block is mainly

*Corresponding author. Email: liushen@vip.gyig.ac.cn

ISSN 0020-6814 print/ISSN 1938-2839 online

http://dx.doi.org/10.1080/00206814.2012.707003
http://www.tandfonline.com

composed of two sequences of Precambrian metamorphic rocks: the Mashan and Heilongjiang groups (Wu *et al*. 2003a, 2003b). The Mashan Group, which has experienced metamorphism to granulite-facies conditions (Wilde *et al*. 2000), comprises granulite, marble, and graphitic schist, together with gneiss and garnet-bearing granite. By contrast, the Heilongjiang Group, exposed along the Mudanjiang Fault zone between the Jiamusi and Songliao blocks, is characterized by highly deformed, blueschist-facies rocks, including glaucophane schist, marble, and chert (Wu *et al*. 2003a, 2003b). The Songliao Block consists of the Lesser Xing'an Range in the north, the Songliao sedimentary basin in the central part, and the Zhangguangcai Range in the east. Voluminous Phanerozoic granitic rocks are widespread throughout the Songliao Block, intruding the mountainous regions (JBGMR 1988; IMBGMR 1990; HBGMR 1993) and beneath the Songliao basins (Wu *et al*. 2001). Furthermore, Proterozoic metamorphic rocks with banded iron formation (Dongfengshan Group) occur within the eastern Lesser Xing'an and northern Zhangguangcai ranges (HBGMR 1993; Wu *et al*. 2003a, 2003b). The Xing'an Block is located within the Great Xing'an Range, where extensive Mesozoic volcanic and granitic rocks are exposed, as are Proterozoic metamorphic rocks and Palaeozoic strata (HBGMR 1993; Wu *et al*. 2003a, 2003b).

The study area for our samples is located close to Dalian, eastern Northeast China (Figures 1A and 1B). Here, Mesozoic dikes outcrop as dolerite intruding Sinian sedimentary strata; the studied mafic rocks are neither deformed nor metamorphosed. The individual mafic dikes are vertical and NW–NE-trending. They are commonly 1.6–6.0 km wide and 10–40 km long (Figure 1B). Representative photomicrographs of the mafic dikes from the studied area are provided in Figure 2. The dolerite dike rocks are typically intermediate to coarse grained and porphyritic, comprising 35–45% phenocrysts of clinopyroxene (3.0–5.5 mm), plagioclase (3.0–4.5 mm), minor K-feldspar (2.5–5.0 mm) and magnetite in a matrix of clinopyroxene (0.05–0.8 mm), plagioclase (0.04–0.06 mm), K-feldspar (0.02–0.04 mm), minor biotite (0.03–0.05 mm), and Ti–Fe oxides (e.g. magnetite) (0.04–0.06 mm).

3. Analytical methods

3.1. Zircon LA–ICP–MS U–Pb dating

Zircon was separated from one of the Dalian dolerite dike samples (YJC-1), using conventional heavy liquid and magnetic techniques, at the Langfang Regional Geological Survey, Hebei Province, China. Representative grains were hand-picked under a binocular microscope, mounted in an epoxy resin disc, and then polished and coated with a conductive film of gold. Zircon grains were observed with transmitted and reflected light microscopy as well as cathodoluminescence (CL) imagery to help reveal their external and internal structures (Figure 3). Microscopic observations were undertaken at the State Key Laboratory of Continental Dynamics, Northwest University, China. Laser ablation techniques were used for zircon age determinations (Table 1). The analyses were conducted with an Agilent 7500a inductively coupled plasma–mass spectrometer (ICP–MS) equipped with 193 nm excimer lasers, which is housed at the State Key Laboratory of Geological Processes and Mineral Resources, China University of Geoscience in Wuhan, China. Zircon 91500 was used as a standard and NIST 610 was used to optimize the results. The spot diameter was 24 μm. Analytical methodology is described in detail in Yuan *et al*. (2004). Common Pb corrections were made using the method of Andersen (2002). Data were processed using the GLITTER and ISOPLOT (Ludwig 2003) programs. Errors on individual analyses by LA–ICP–MS are quoted at the 95% (1σ) confidence level.

3.2. Major and trace elemental analyses

Fifteen mafic dike samples were selected to carry out major and trace element determinations and Sr–Nd isotopic analyses. Whole-rock samples were trimmed to remove altered surfaces, and were cleaned with deionized water, crushed, and powdered with an agate mill.

Major elements were analysed with a PANalytical Axios-Advanced PW4400 X-ray fluorescence spectrometer (XRF) at the State Key Laboratory of Ore Deposit Geochemistry, Institute of Geochemistry, Chinese Academy of Sciences (IGCAS), China. Fused glass discs were used and the analytical precision, as determined on the Chinese national geological rock standards GSR-1 and GSR-3, was better than 3% (Table 2). Loss on ignition (LOI; Table 2) was obtained using 1 g of powder heated up to 1100°C for 1 h.

Trace element concentrations were determined with an ELAN 6000 ICP–MS at IGCAS following the procedures described by Qi *et al*. (2000). The discrepancy between triplicate analyses is less than 5% for all elements. Analysis of international standard GBPG-1 (plagiogneiss) is in agreement with recommended values (Table 3).

3.3. Sr–Nd isotopic analyses

For Rb–Sr and Sm–Nd isotopic analysis, sample powders were spiked with mixed isotope tracers, dissolved in Teflon capsules with HF + HNO_3 acids, and separated by conventional cation-exchange techniques. Isotopic measurements were performed on a Finnigan MAT-261 thermal ionization mass spectrometer (TIMS) at the State Key Laboratory of Geological Processes and Mineral Resources, China University of Geosciences, China. Procedural blanks were <200 pg for Sm and Nd and <500 pg for Rb and Sr. The mass fractionation corrections for Sr and Nd

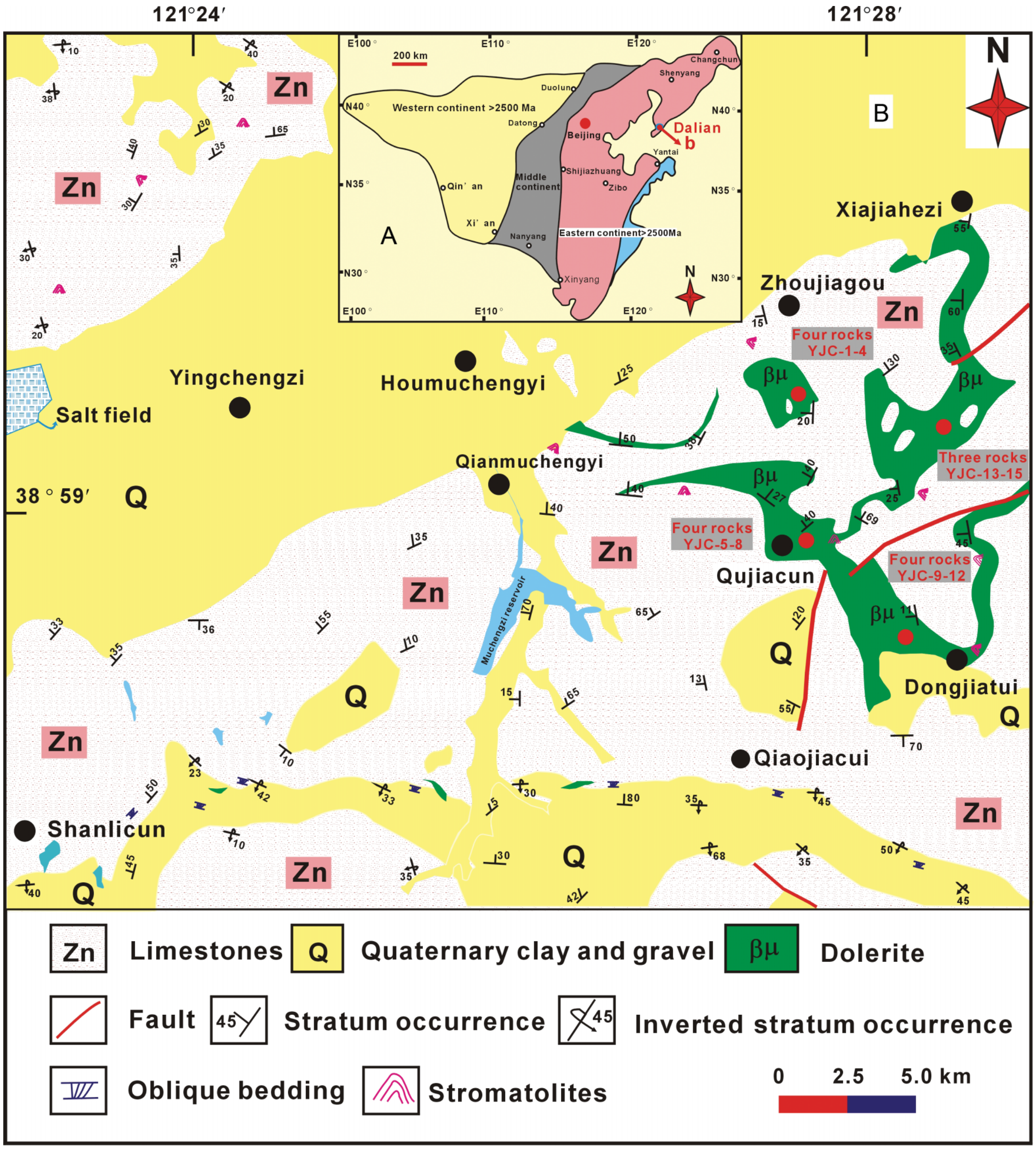

Figure 1. (A) Location of the study area (highlighted in (B)), close to the city of Dalian, China. (B) Geological map of the study area including the sampling localities for the investigated mafic dikes.

isotopic ratios were based on $^{86}Sr/^{88}Sr = 0.1194$ and $^{146}Nd/^{144}Nd = 0.7219$, respectively. Analyses of standards during the period of analysis are as follows: NBS987 gave $^{87}Sr/^{86}Sr = 0.710248 \pm 12$ (2σ, $n = 10$) and La Jolla gave $^{143}Nd/^{144}Nd = 0.511856 \pm 10$ (2σ, $n = 10$). Our analytical results for Sr–Nd isotopes are presented in Table 4.

3.4. In situ *zircon Hf isotopic analysis*

In situ zircon Hf isotopic analyses were conducted using a Neptune MC–ICP–MS, equipped with a 193 nm laser, at the Institute of Geology and Geophysics, Chinese Academy of Sciences in Beijing, China. During the analysis, a laser repetition rate of 10 Hz at 100 mJ and spot sizes of 32 and 63 μm were used. Details of the analytical technique used are given in Xu *et al*. (2004) and Wu *et al*. (2006). During the analysis, the $^{176}Hf/^{177}Hf$ and $^{176}Lu/^{177}Hf$ ratios of the standard zircon (91500) were 0.282300 ± 15 ($2\sigma n$, $n = 24$) and 0.00030, similar to the commonly accepted $^{176}Hf/^{177}Hf$ ratio of 0.282302 ± 8 and 0.282306 ± 8 (2σ), measured using the solution method (Goolaerts *et al*. 2004; Woodhead *et al*. 2004). The analytical results are presented in Table 5.

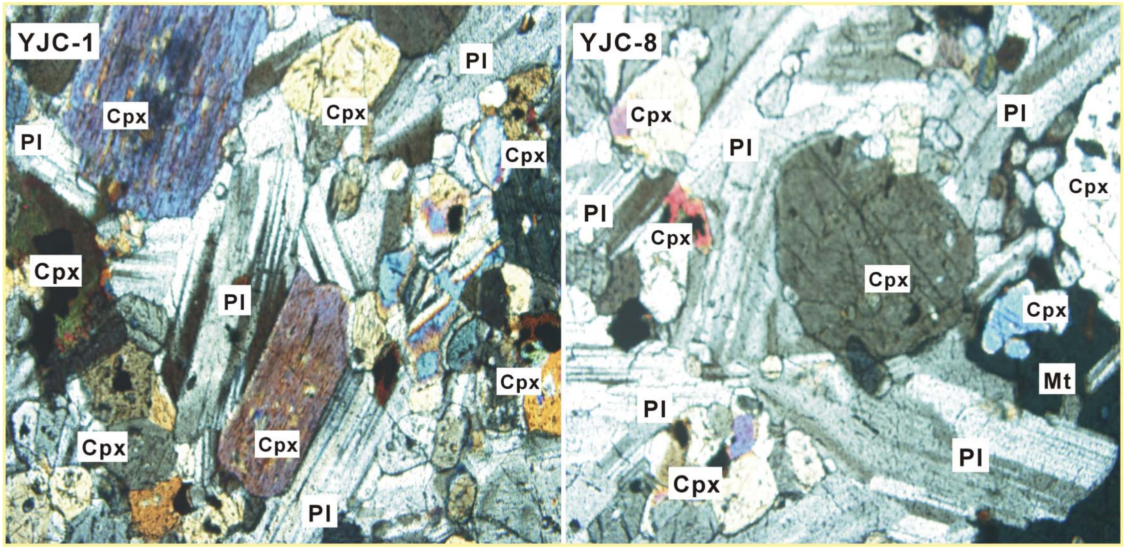

Figure 2. Representative photomicrographs of the mafic dikes from Dalian, Northeast China (cross-polarized light). Cpx, clinopyroxene; Pl, plagioclase feldspar.

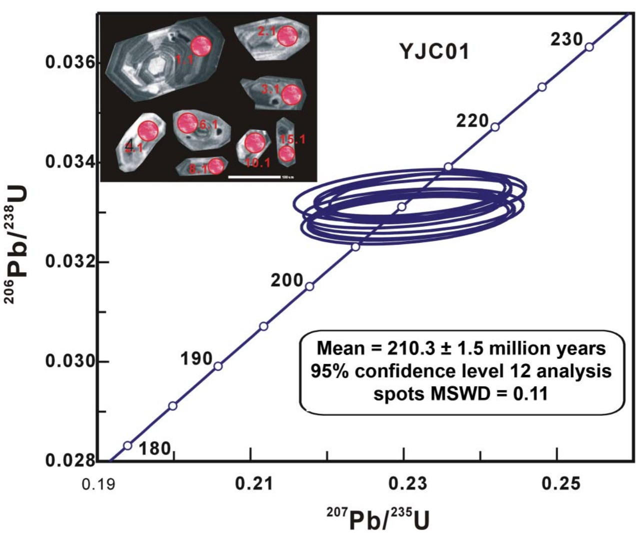

Figure 3. Representative cathodoluminescence images and LA–ICP–MS U–Pb concordia diagrams of zircon grains from the investigated mafic dike sample YJC-1. The numbers on individual zircon grains correspond to the locations of spot analyses given in Table 1. MSWD, mean square of weighted deviates.

4. Results

4.1. *Zircon CL imagery and U–Pb data*

Zircon is relatively abundant in mafic dike YJC-1. Prior to LA–ICP–MS zircon U–Pb dating, the surfaces of the grain mounts were washed in dilute HNO_3 and pure alcohol to remove any potential lead contamination. Zircons selected from sample YJC-1 are euhedral, colourless, and transparent; mostly elongated prismatic; and range up to 100 μm in diameter. The majority of grains exhibited oscillatory or planar zoning under CL, a typical feature of magmatic zircon (see Figure 3). The studied zircon grains have variable abundances of Th (30.5–526 ppm) and U (52.7–502 ppm), with variable Th/U ratios (0.52–4.47) (Table 1), also suggestive of a magmatic origin. On the basis of petrographic and CL examination and Th/U ratios, an igneous origin for the zircon from dike YJC-1 is evident. The U–Pb zircon data are presented in Table 1. Analyses of zircon grains with oscillatory structures were concordant and yielded a weighted mean $^{206}Pb/^{238}U$ age of 210.3 ± 1.5 million years ($n = 12$) for YJC-1 (Figure 3). The age is interpreted as the crystallization age of the dolerite intrusion.

4.2. *Major and trace elements*

Major element concentrations of the studied mafic samples are presented in Table 2. The mafic dikes have a small range of chemical compositions, with $SiO_2 = 47.24–48.50$ wt.%, $Al_2O_3 = 14.87–15.89$ wt.%, $Fe_2O_3 = 12.52–13.84$ wt.%, $MgO = 4.65–5.44$ wt.%, $CaO = 9.21–10.43$ wt.%, $Na_2O = 2.56–3.31$ wt.%, $K_2O = 0.84–1.23$ wt.%, $MnO = 0.15–0.20$ wt.%, $P_2O_5 = 0.28–0.36$ wt.%, and $TiO_2 = 2.42–2.93$ wt.%, as well as a narrow spread in $Mg^{\#}$ values (41–44). Most mafic rocks fall along the boundary between alkaline and calc-alkaline rock associations in the total alkali-silica (TAS) diagram (Figure 4A). In addition, almost all of the samples straddle the intersections of calc-alkaline and shoshonitic series in the Na_2O versus K_2O plot (Figure 4B). In a plot of molar ratios of $Al_2O_3/(Na_2O + K_2O)$ and $Al_2O_3/(CaO + Na_2O + K_2O)$, the mafic rocks are all metaluminous (Figure 4C). Harker diagrams (Figure 5) show the variation in major elements as a function of MgO content in the mafic rocks. With increasing MgO content, Al_2O_3, TiO_2, Na_2O, and P_2O_5 decrease, whereas Fe_2O_3, CaO, and K_2O increase. Trace element concentrations of the mafic dikes are presented in

Table 1. LA–ICP–MS U–Pb isotopic data for zircon from the mafic dikes in Dalian, China.

					Isotopic ratios						Age (million years)					
YJC-1 spot	Th (ppm)	U (ppm)	Pb (ppm)	Th/U (ppm)	$^{207}Pb/^{206}Pb$	1σ	$^{207}Pb/^{235}U$	1σ	$^{206}Pb/^{238}U$	1σ	$^{207}Pb/^{206}Pb$	1σ	$^{207}Pb/^{235}U$	1σ	$^{206}Pb/^{238}U$	1σ
1.1	107	143	23.6	0.75	0.0552	0.0046	0.2941	0.0080	0.0330	0.0003	419	190	228	17	210	3
2.1	235	391	18.1	0.60	0.0547	0.0022	0.2942	0.0081	0.0332	0.0003	400	88	227	10	211	2
3.1	62.0	93.2	18.8	0.67	0.0555	0.0016	0.2306	0.0092	0.0329	0.0003	433	51	308	10	209	4
4.1	261	502	21.7	0.52	0.0502	0.0026	0.2299	0.0085	0.0331	0.0003	202	119	209	10	210	2
5.1	73.6	91.5	16.2	0.80	0.0585	0.0017	0.2306	0.0087	0.0329	0.0003	547	78	294	13	209	4
6.1	137	251	51.4	0.54	0.0526	0.0014	0.2309	0.0088	0.0330	0.0003	309	56	218	6	209	2
7.1	146	167	14.6	0.88	0.0551	0.0022	0.2316	0.0093	0.0330	0.0003	416	115	247	15	209	4
8.1	113	155	34.4	0.73	0.0665	0.0032	0.2299	0.0094	0.0334	0.0003	823	89	279	13	211	3
9.1	302	408	22.1	0.74	0.0518	0.0025	0.2308	0.0082	0.0334	0.0003	278	114	217	9	211	2
10.1	30.5	52.7	17.0	0.58	0.0676	0.0026	0.2332	0.0085	0.0333	0.0003	855	76	306	12	211	3
11.1	405	411	24.3	0.99	0.0562	0.0012	0.2321	0.0091	0.0333	0.0003	459	53	283	9	211	3
12.1	526	357	25.1	1.47	0.0528	0.0023	0.2314	0.0084	0.0333	0.0003	319	97	222	11	211	3

Table 2. Whole-rock determinations of major elements (oxide wt.%) for the mafic dikes in Dalian, China.

Sample no.	SiO_2	Al_2O_3	Fe_2O_3	MgO	CaO	Na_2O	K_2O	MnO	P_2O_5	TiO_2	LOI	Total	$Mg^{\#}$
YJC-1	48.05	15.89	13.51	4.77	9.40	2.93	1.23	0.19	0.35	2.59	1.99	100.90	41.4
YJC-2	47.70	15.62	13.44	5.32	10.24	2.73	1.13	0.19	0.33	2.50	1.52	100.72	44.2
YJC-3	47.60	15.41	13.72	5.33	9.89	2.65	1.18	0.19	0.34	2.57	1.87	100.74	43.7
YJC-4	47.24	15.32	13.84	4.96	9.69	3.19	0.98	0.20	0.36	2.91	2.09	100.77	41.8
YJC-5	48.23	15.03	13.48	5.29	10.14	2.76	1.13	0.19	0.33	2.42	1.92	100.91	44.0
YJC-6	47.69	15.33	13.64	5.44	10.43	2.74	1.12	0.19	0.32	2.57	1.51	100.97	44.4
YJC-7	48.50	15.33	13.48	4.91	9.21	3.31	0.94	0.19	0.35	2.66	2.04	100.91	42.1
YJC-8	47.25	15.60	13.54	4.87	9.53	3.19	1.02	0.20	0.34	2.93	2.19	100.66	41.8
YJC-9	48.13	15.54	13.16	4.99	9.89	2.96	0.98	0.19	0.33	2.49	2.09	100.75	43.1
YJC-10	47.88	14.91	12.52	4.65	10.01	2.56	0.84	0.18	0.31	2.58	2.07	98.51	42.6
YJC-11	47.76	15.37	13.34	5.28	10.16	2.67	1.08	0.17	0.31	2.47	1.53	99.88	42.8
YJC-12	47.85	14.87	13.42	5.23	9.93	2.58	1.03	0.15	0.28	2.43	1.48	99.75	42.7
YJC-13	48.26	14.98	13.46	5.26	10.12	2.72	1.11	1.10	0.31	2.86	2.03	99.62	42.7
YJC-14	48.18	15.49	13.13	4.92	9.85	2.93	0.95	0.17	0.32	2.65	2.04	99.49	42.7
YJC-15	47.73	15.57	13.41	5.31	10.21	2.71	1.12	0.18	0.32	2.48	1.47	99.36	42.7
GSR-3	RV*	44.64	13.83	13.4	7.77	8.81	3.38	2.32	0.17	0.95	2.37	2.24	99.88
GSR-3	MV*	44.68	13.98	13.37	7.75	8.82	3.26	2.31	0.17	0.96	2.36	2.15	99.81
GSR-1	RV*	72.83	13.4	2.14	0.42	1.55	3.13	5.01	0.06	0.09	0.29	0.7	99.62
GSR-1	MV*	72.76	13.43	2.16	0.43	1.57	3.16	5.02	0.06	0.1	0.29	0.71	99.69

Notes: LOI, loss on ignition; $Mg^{\#}$, 100 × Mg/(Mg + ΣFe) atomic ratio; RV*, recommended values; MV*, measured values. The recommended values quoted for standards GSR-1 and GSR-3 are from Wang *et al*. (2003).

Table 3. Selected elements are plotted against MgO content in Figure 6. Rb, Sr, and Zr concentrations decrease, whereas Ba, Cr, and Ni concentrations increase with increasing MgO. All samples have moderate total rare earth element (REE) contents (113–137 ppm). The mafic dikes have relatively larger variation in $(La/Yb)_N$ (4.9–5.8), $(Gd/Yb)_N$ (1.7–1.9), and Eu/Eu* (1.01–1.17), and are characterized by relatively high Nb (18.5–24.5 ppm), Y (29–36 ppm), Sr (306–392 ppm), Ba (241–349 ppm), and Sc (30–33 ppm) contents and low Rb (25–36 ppm), Zr (135–173 ppm), Hf (3.4–4.4 ppm), U (0.4–0.7 ppm), Th (2.2–2.7 ppm), and Pb (6.6–14 ppm) contents (Table 3). In primitive mantle-normalized multi-element diagrams (Figure 7B), the mafic samples exhibit enrichment in Rb, Ba, U, K, and Pb and significant depletions in Th, Nb, and Ti (Figure 7B).

4.3. Sr–Nd isotopes

Sr and Nd isotopic compositions of the representative samples from mafic dikes are presented in Table 4. The mafic dikes have relatively constant initial $^{87}Sr/^{86}Sr$ ratios (0.7061–0.7067) and negative ε_{Nd} (t) values (−4.7 to −4.3). Furthermore, in the $(^{87}Sr/^{86}Sr)_i$ versus ε_{Nd} (t) plot (Figure 8), the mafic dikes fall within the field of an enriched mantle source.

4.4. Zircon Hf isotopes

One sample of zircon dated by U–Pb methods was also studied for its Lu–Hf isotopic signature, with analyses made on the same domains, and the results are presented in Table 5. Sixteen spot analyses were obtained for the zircon in sample YJC-1, yielding variable ε_{Hf} (t) values of between −4.1 and −1.1 (Figure 9), two-stage model ages (TDM2) of 1312–1503 million years, and initial $^{176}Hf/^{177}Hf$ ratios ranging from 0.282542 to 0.282593.

5. Discussion

5.1. Petrogenesis

5.1.1. Source regions

The Dalian area mafic dikes exhibit lower SiO_2 contents (47.24–48.50 wt.%) than the liquids that would result from partial melting of any of the crustal rocks (i.e. granitoid liquids; e.g. Hirajima *et al*. 1990; Yang *et al*. 1993; Zhang *et al*. 1994; Kato *et al*. 1997; Gao *et al*. 1998a, 1998b; Rapp *et al*. 2003), suggesting that the dikes are derived from a mantle rather than a crustal source. Moreover, the high initial $^{87}Sr/^{86}Sr$ (0.7061–0.7067) ratios and negative ε_{Nd} (t) (−4.7 to −4.3) and zircon ε_{Hf} (t) (−4.1 to −1.1) values (Tables 4 and 5; Figures 8 and 9) for the mafic rocks are consistent with derivation from an enriched, lithospheric, mantle source.

5.1.2. Crustal assimilation

The investigated mafic dikes display positive Pb and negative Ti anomalies when plotted on multi-element, normalized spider diagrams (Figure 7B), suggesting that continental material could have played a role in the magma

Table 3. Trace elements (ppm) for the mafic dikes in Dalian, China.

Sample	YJC-1	YJC-2	YJC-3	YJC-4	YJC-5	YJC-6	YJC-7	YJC-8	YJC-9	YJC-10	YJC-11	YJC-12	YJC-13	YJC-14	YJC-15	GBPG-1 (RV*)	GBPG-1 (MV*)
Sc	30.5	31.0	31.2	33.2	31.0	33.6	32.4	31.2	30.3	33.1	30.8	30.3	30.8	30.1	30.6	13.9	14.3
V	345	347	324	351	299	383	367	390	342	395	343	336	293	335	346	96.5	101
Cr	95.4	122	123	100	119	125	97.9	89.9	106	107	118	112	114	103	122	19.5	20.1
Ni	61.6	70.5	66.2	64.7	69.9	72.2	56.7	60.2	63.4	66.4	68.8	67.5	67.6	62.8	70.5	18.6	19.2
Rb	35.3	27.6	31.0	30.7	27.7	29.4	29.3	30.7	28.0	25.9	26.8	25.5	26.7	27.6	27.4	56.2	55.8
Sr	359	319	310	382	326	315	381	378	392	385	312	306	317	388	315	364	367
Y	35.7	30.7	30.7	33.7	31.6	29.9	34.6	32.4	32.0	31.1	30.4	29.7	30.9	31.5	30.7	18	18.4
Zr	165	145	149	167	152	150	170	173	148	160	139	135	146	142	143	232	232
Nb	22.5	19.7	20.4	23.9	19.7	21.1	23.9	24.5	20.9	22.4	19.4	18.5	19.3	20.3	20.2	9.93	10.2
Ba	308	349	344	264	327	320	248	313	248	242	341	332	323	241	345	908	916
La	24.2	20.9	20.2	22.9	20.8	19.1	22.7	21.0	21.6	21.2	20.5	19.6	19.5	21.3	21.2	53.0	55.0
Ce	48.2	44.0	42.3	48.9	42.3	40.1	47.6	44.4	44.9	43.8	43.5	42.1	41.6	43.9	44.3	103	98.7
Pr	6.32	5.72	5.35	6.20	5.49	5.16	6.14	5.92	5.82	5.83	5.66	5.5	5.42	5.76	5.71	11.5	11.9
Nd	28.7	25.9	24.3	27.1	24.6	22.7	27.3	26.0	25.1	25.3	25.2	24.8	23.5	24.6	25.4	43.3	43.1
Sm	6.19	5.52	5.30	6.11	5.62	5.18	5.95	5.65	5.58	5.66	5.48	5.35	5.57	5.54	5.55	6.79	6.97
Eu	2.32	1.93	1.88	2.12	2.03	1.84	2.17	2.22	2.02	2.06	1.89	1.83	1.96	1.97	1.93	1.79	1.84
Gd	6.31	5.87	5.59	6.48	6.04	5.55	6.40	5.97	5.88	5.96	5.83	5.74	5.83	5.82	5.86	4.74	4.75
Tb	0.96	0.88	0.88	0.99	0.90	0.89	0.99	0.97	0.90	0.90	0.84	0.82	0.88	0.85	0.86	0.6	0.63
Dy	5.88	5.58	5.23	6.24	5.55	5.41	5.82	5.97	5.73	5.64	5.52	5.43	5.53	5.66	5.57	3.26	3.18
Ho	1.16	1.09	1.07	1.19	1.08	1.04	1.17	1.16	1.11	1.11	1.05	1.02	1.06	1.08	1.07	0.69	0.71
Er	3.04	2.83	2.86	3.13	2.82	2.80	3.19	3.07	2.86	2.84	2.76	2.69	2.81	2.77	2.83	2.01	2.03
Tm	0.42	0.38	0.36	0.42	0.38	0.38	0.43	0.42	0.37	0.37	0.36	0.33	0.36	0.35	0.38	0.3	0.31
Yb	2.93	2.58	2.43	2.83	2.69	2.54	2.80	2.77	2.54	2.69	2.53	2.41	2.65	2.48	2.55	2.03	2.1
Lu	0.43	0.38	0.36	0.43	0.39	0.39	0.40	0.40	0.39	0.40	0.36	0.34	0.38	0.36	0.37	0.31	0.31
Hf	4.03	3.63	3.49	3.96	3.65	3.70	4.35	4.02	3.81	4.14	3.57	3.43	3.63	3.73	3.66	6.07	5.92
Ta	1.52	1.31	1.28	1.50	1.18	1.34	1.44	1.51	1.35	1.44	1.27	1.24	1.16	1.25	1.31	0.4	0.39
Pb	6.61	10.4	9.89	9.13	14.2	12.22	9.46	9.60	9.48	7.81	9.96	9.78	13.8	9.41	10.2	14.1	13.6
Th	2.66	2.34	2.30	2.59	2.36	2.25	2.60	2.51	2.29	2.26	2.28	2.25	2.33	2.24	2.32	11.2	11.4
U	0.60	0.67	0.50	0.65	0.57	0.70	0.60	0.67	0.50	0.66	0.63	0.56	0.55	0.48	0.65	0.9	0.87
δEu	1.13	1.03	1.06	1.03	1.06	1.05	1.07	1.17	1.08	1.08	1.02	1.01	1.05	1.06	1.03		

Note: The values for GBPG-1 are from Thompson *et al*. (2000).

Table 4. Sr–Nd isotopic compositions of the mafic dikes in Dalian, China.

Sample	Age (million years)	Rb (ppm)	Sr (ppm)	$^{87}Rb/^{86}Sr$	$^{87}Sr/^{86}Sr$	2σ	$(^{87}Sr/^{86}Sr)_i$	Sm (ppm)	Nd (ppm)	$^{147}Sm/^{144}Nd$	$^{143}Nd/^{144}Nd$	2σ	$(^{143}Nd/^{144}Nd)_i$	$\epsilon_{Nd}(t)$
YJC-1		35.3	359	0.2842	0.706968	8	0.706168	6.19	28.7	0.1304	0.512316	8	0.512137	−4.5
YJC-2		27.6	319	0.2500	0.706573	10	0.706573	5.52	25.9	0.1288	0.512323	9	0.512323	−4.3
YJC-3		31.0	310	0.2890	0.706712	12	0.706712	5.30	24.3	0.1318	0.512321	9	0.512321	−4.4
YJC-5	210.3	27.7	326	0.2456	0.706989	10	0.706255	5.62	24.6	0.1381	0.512320	12	0.512130	−4.6
YJC-9		28.0	392	0.2064	0.706726	8	0.706109	5.58	25.1	0.1344	0.512313	9	0.512128	−4.7
YJC-10		25.9	385	0.1944	0.706451	8	0.706451	5.66	25.3	0.1352	0.512314	9	0.512314	−4.7
YJC-12		25.5	306	0.2408	0.706659	10	0.706659	5.35	24.8	0.1304	0.512313	8	0.512313	−4.6
YJC-15		25.5	306	0.2408	0.706659	8	0.706659	5.35	24.8	0.1034	0.512314	10	0.512314	−4.5

Notes: Chondrite uniform reservoir (CHUR) values ($^{87}Rb/^{86}Sr = 0.0847$, $^{87}Sr/^{86}Sr = 0.7045$, $^{147}Sm/^{144}Nd = 0.1967$, and $^{143}Nd/^{144}Nd = 0.512638$) are used for the calculation. $\lambda_{Rb} = 1.42 \times 10^{-11}$ year^{-1} (Steiger and Jäger 1977); $\lambda_{Sm} = 6.54 \times 10^{-12}$ year^{-1} (Lugmair and Harti 1978).

Table 5. Zircon Hf isotopic compositions of the mafic dikes from Dalian, China.

No.	$^{176}Yb/^{177}Hf$	2σ	$^{176}Lu/^{177}Hf$	2σ	$^{176}Hf/^{177}Hf$	2σ	Age (million years)	$^{176}Hf/^{177}Hf$	$\varepsilon_{Hf}(0)$	$\varepsilon_{Hf}(t)$	T_{DM1} (million years)	T_{DM2} (million years)	$f_{Lu/Hf}$
1	0.026148	0.000687	0.001035	0.000029	0.282535	0.000028	210.3	0.282531	−8.4	−3.9	1017	1492	−0.97
2	0.030847	0.001246	0.001256	0.000052	0.282594	0.000036	210.3	0.282589	−6.3	−1.9	939	1361	−0.96
3	0.013685	0.000322	0.000490	0.000015	0.282540	0.000031	210.3	0.282538	−8.2	−3.7	996	1477	−0.99
4	0.022244	0.000335	0.000872	0.000014	0.282529	0.000028	210.3	0.282526	−8.6	−4.1	1020	1503	−0.97
5	0.037865	0.000364	0.001574	0.000017	0.282539	0.000028	210.3	0.282533	−8.2	−3.8	1025	1487	−0.95
6	0.034675	0.000832	0.001436	0.000016	0.282560	0.000033	210.3	0.282554	−7.5	−3.1	992	1440	−0.96
7	0.042136	0.001124	0.001653	0.000038	0.282586	0.000026	210.3	0.282580	−6.6	−2.2	960	1383	−0.95
8	0.035564	0.000624	0.001484	0.000026	0.282572	0.000028	210.3	0.282566	−7.1	−2.7	976	1412	−0.96
9	0.015421	0.000832	0.000606	0.000013	0.282595	0.000026	210.3	0.282593	−6.3	−1.7	921	1353	−0.98
10	0.028986	0.000747	0.001286	0.000022	0.282574	0.000027	210.3	0.282569	−7.0	−2.6	967	1406	−0.96
11	0.018237	0.000857	0.000674	0.000014	0.282594	0.000027	210.3	0.282591	−6.3	−1.8	925	1357	−0.98
12	0.023367	0.000864	0.000893	0.000015	0.282577	0.000030	210.3	0.282573	−6.9	−2.4	954	1397	−0.97
13	0.027413	0.000257	0.001214	0.000017	0.282557	0.000025	210.3	0.282552	−7.6	−3.2	990	1444	−0.96
14	0.036739	0.000657	0.001234	0.000025	0.282593	0.000028	210.3	0.282589	−6.3	−1.9	939	1363	−0.96
15	0.031558	0.000383	0.001225	0.000031	0.282547	0.000025	210.3	0.282542	−8.0	−3.5	1004	1467	−0.96
16	0.353892	0.000683	0.001237	0.000026	0.282616	0.000029	210.3	0.282611	−5.52	−1.1	907	1312	−0.96

Notes: $\varepsilon_{Hf}(t) = 10{,}000\{[(^{176}Hf/^{177}Hf)_S - (^{176}Lu/^{177}Hf)_S \times (e^{\lambda t} - 1)]/[(^{176}Hf/^{177}Hf)_{CHUR,0} - (^{176}Lu/^{177}Hf)_{CHUR} \times (e^{\lambda t} - 1)] - 1\}$.

$T_{DM^*} = 1/\lambda \times \ln\{1 + (^{176}Hf/^{177}Hf)_S - (^{176}Hf/^{177}Hf)_{DM}]/[(^{176}Lu/^{177}Hf)_S - (^{176}Lu/^{177}Hf)_{DM}]\}$.

$T^C_{DM} = 1/\lambda \times \ln\{1 + [(^{176}Hf/^{177}Hf)_{S,t} - (^{176}Hf/^{177}Hf)_{DM,t}]/[(^{176}Lu/^{177}Hf)_C - (^{176}Lu/^{177}Hf)_{DM}]\} + t$.

The $^{176}Hf/^{177}Hf$ and $^{176}Lu/^{177}Hf$ ratios of chondrite and depleted mantle at present are 0.282772 and 0.0332, and 0.28325 and 0.0384, respectively (Blichert-Toft and Albare'de 1997; Griffin *et al*. 2000). $\lambda = 1.867 \times 10^{-11}$ year^{-1} (Soderlund *et al*. 2004). $(^{176}Lu/^{177}Hf)_C = 0.015$, t = crystallization age of zircon.

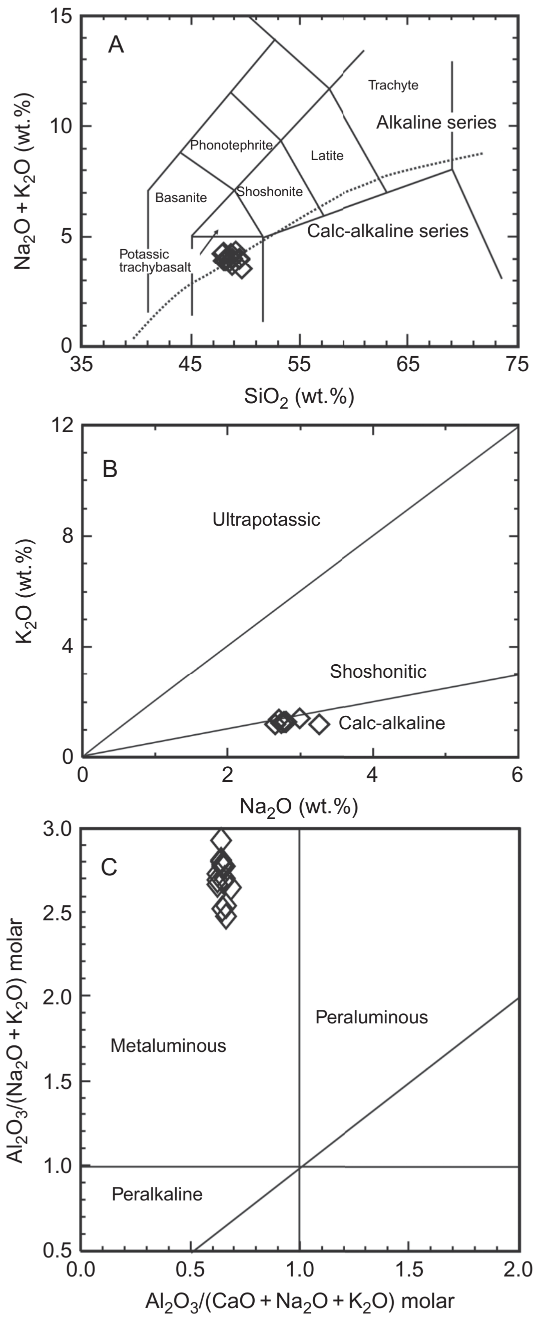

Figure 4. Classification of the Dalian area mafic dikes based upon the following three diagrams. (A) TAS diagram. All major elemental data have been recalculated to 100% on an LOI-free basis [after Middlemost (1994) and Le Maitre (2002)]. (B) K_2O versus Na_2O diagram. The mafic dikes are shown to be calc-alkaline to marginally shoshonitic in character [after Middlemost (1972)]. (C) $Al_2O_3/(Na_2O + K_2O)$ molar versus $Al_2O_3/(CaO + Na_2O + K_2O)$ molar plot. All samples fall in the field of metaluminous rocks.

genesis of these rocks. Crustal contamination might cause significant depletion in Nb–Ta and highly enriched Sr–Nd isotopic signatures in basaltic rocks (Guo *et al*. 2004a, 2004b). The mafic dikes are characterized by negative

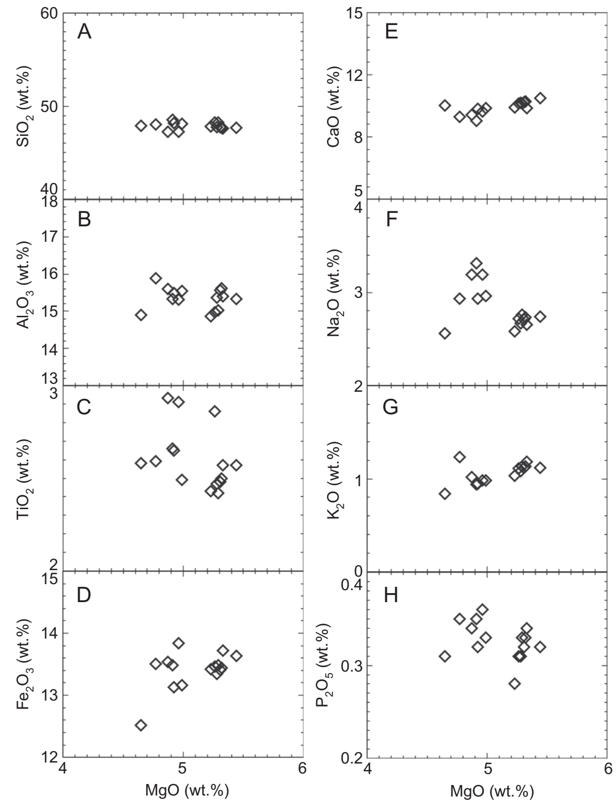

Figure 5. Chemical variation diagrams (A–H) of whole-rock major elements versus MgO content for the mafic dikes in this study.

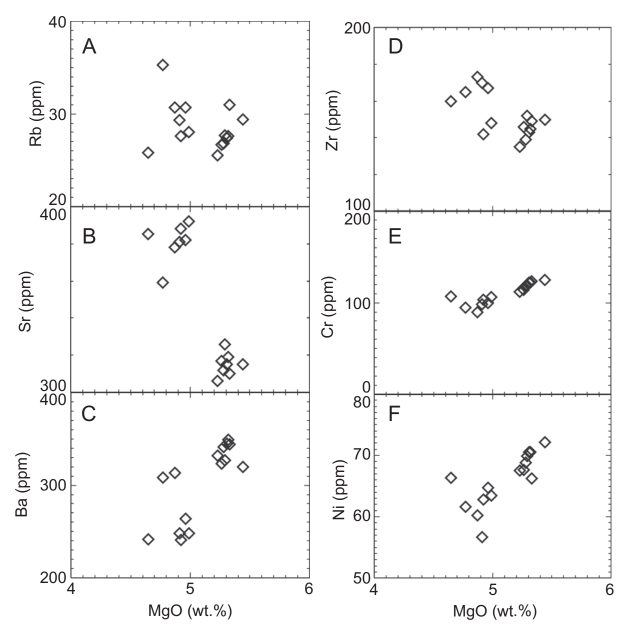

Figure 6. Variation diagrams (A–F) of selected trace elements versus MgO for the mafic dikes in this study.

Nb anomalies, high and constant initial $^{87}Sr/^{86}Sr$ ratios, and negative ε_{Nd} (t) values (Table 4; Figure 8), implying

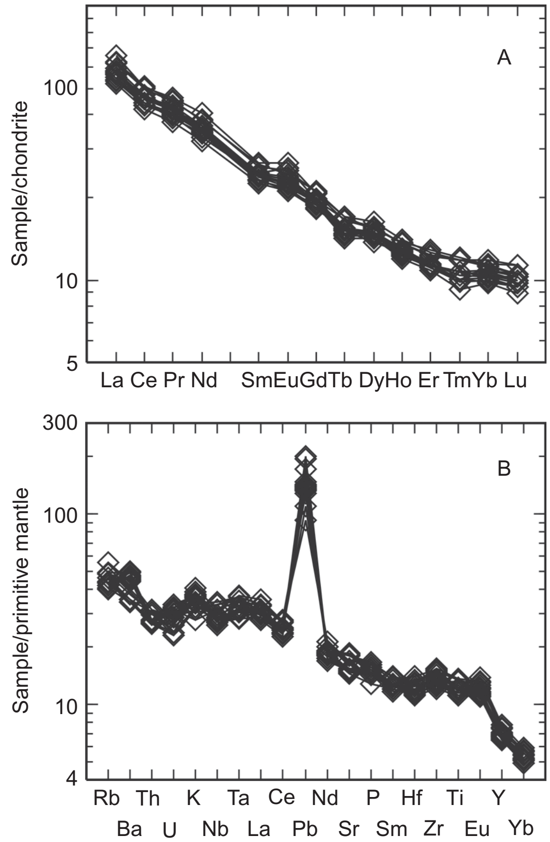

Figure 7. Chondrite-normalized whole-rock (A) rare earth element and (B) primitive mantle-normalized spider patterns for the mafic dikes in this study. REE abundances for chondrite and trace element abundance for primitive mantle are taken from Sun and McDonough (1989).

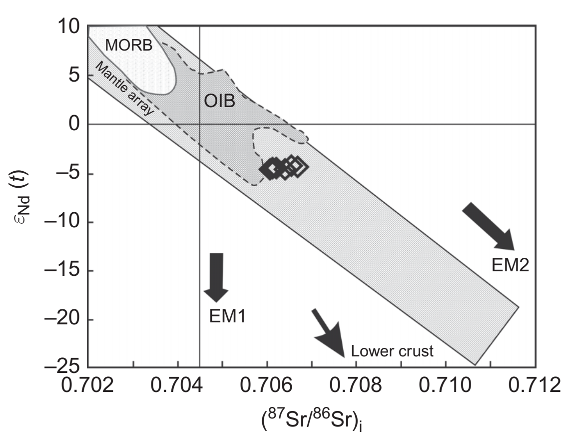

Figure 8. ε_{Nd} (t) versus $(^{87}Sr/^{86}Sr)_i$ diagram of the mafic dikes in this study. Mid-ocean ridge basalt (MORB) and ocean island basalt (OIB) are taken from Zhang *et al*. (2002) and the references therein; mantle array is taken from Zhang *et al*. (2005); EM1, EM2, and lower crust are taken from Jahn *et al*. (1999).

that crustal contamination might, therefore, be significant in these rocks. However, crustal assimilation would induce to a certain extent variation in Sr–Nd isotopes,

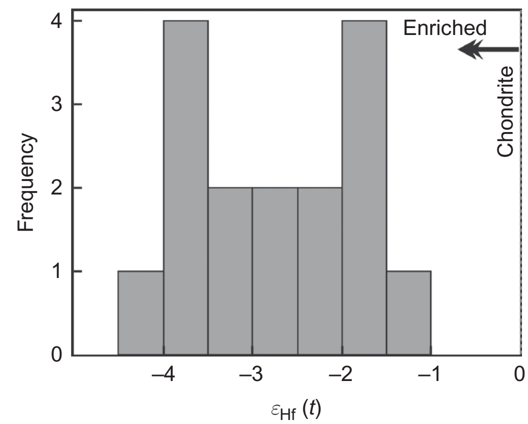

Figure 9. Histograms of ε_{Hf} (t) values of zircon with ages of 210.3 million years in a single mafic dike (YTC-01) from the study area. ε_{Hf} (t) values for the zircons were calculated using the crystallization ages of the mafic rocks.

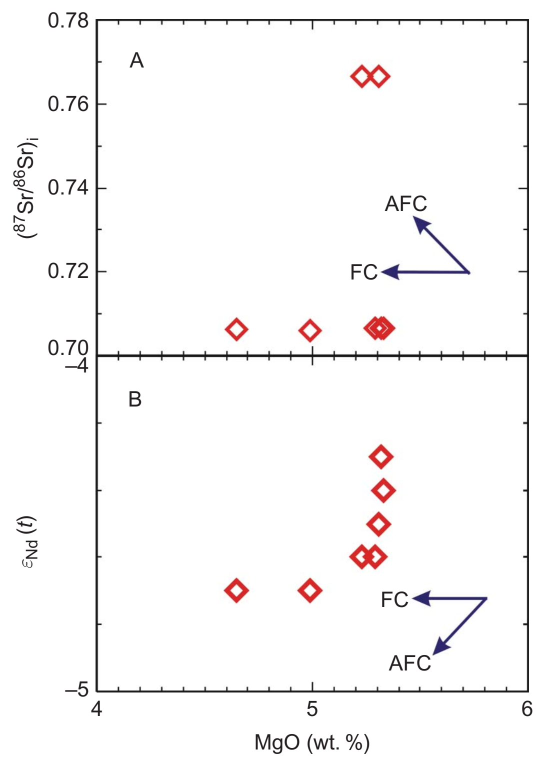

Figure 10. Plots of (A) initial $^{87}Sr/^{86}Sr$ ratio and (B) ε_{Nd} (t) value versus MgO for the mafic dikes in Dalian, Northeast China. FC, fractional crystallization; AFC, assimilation–fractional crystallization.

and also result in a positive correlation between MgO and ε_{Nd} (t) values and a negative correlation between MgO and $(^{87}Sr/^{86}Sr)_i$ ratios. These features, however, are not observed in the studied mafic dikes (Figure 10), which excludes significant assimilation–fractional crystallization (AFC) processes during the later evolution of the mafic magmas. This is further supported by similar Ta/La ratios (0.05–0.07) to that of primitive mantle (i.e. Ta/La = 0.06;

Wood *et al*. 1979). In summary, the geochemical (e.g. positive Pb) and Sr–Nd–Hf isotopic signatures of the Dalian area mafic rocks appear mainly to have been inherited from an enriched mantle source.

5.1.3. *Fractional crystallization*

The observed chemistry of the Dalian area mafic dikes leads to the interpretation that their evolution included some degree of fractional crystallization, as evidenced by low MgO (4.65–5.44 wt.%), $Mg^{\#}$ (41–44) (Table 2), and compatible element content [such as Cr (89–125 ppm) and Ni (56–72 ppm)] (Table 3). The presence of negative correlations between MgO and Al_2O_3, TiO_2, Na_2O, and P_2O_5 (Figures 5B, 5C, 5F, and 5H) and between MgO and Sr and Zr (Figures 6B and 6D) suggests olivine (ol), clinopyroxene (cpx), hornblende (hb), plagioclase (pl), Ti-bearing phases (rutile, ilmenite, titanite, etc.), apatite (ap), and zircon fractionation, while the separation of plagioclase, Ti–Fe oxides, and apatite might account for the observed negative Nb and Ti anomalies in primitive mantle-normalized trace element diagrams (Figure 7B).

5.1.4. *Genetic model*

Based on the above discussion and results, the mafic dikes in this study were likely derived through partial melting of an enriched, lithospheric mantle source. However, the genetic model of these rocks needs to be investigated.

The Mesozoic mafic dikes from Dalian are almost exclusively found to intrude felsic rocks (i.e. granites, granodiorite). Furthermore, these mafic rocks have been proposed to have formed in an extensional setting (Liu *et al*. 2010b). Therefore, in order to account for the genetic model of the mafic dikes, the origin of huge volumes of felsic, granitic rocks in Northeast China also needs to be evaluated. Wu *et al*. (2003b) proposed that the areal distribution of granites may relate to post-orogenic extensional collapse of the Central Asian Orogenic Belt (CAOB), which is called the Xingmeng (Xing'an–Mongolian) Orogenic Belt in the Chinese literature. In other words, granitoid formation was related to massive underplating of mafic magma in an extensional tectonic setting. It has since been suggested that the Central Asian orogeny terminated during the late Palaeozoic (~270 Ma), when collapse and crustal extension occurred (Zhao *et al*. 2008). As crustal extension, in turn, would induce upwelling of hot asthenosphere, it was the high heat flow from this asthenospheric mantle that triggered intense melting in the pre-existing enriched lithospheric mantle, producing voluminous basaltic magmas. Subsequently, these mantle-derived magmas ascended along fractures and faults and arrived into a lower crust; the voluminous granitic magmas were generated by partial melting of pre-existing mixed sources, heated by the underplated basaltic magmas during the late Palaeozoic. Meanwhile, intensive fractionation of the basaltic magma occurred and resulted in the development and emplacement of the Mesozoic (Triassic) mafic dike swarms that have been investigated in this study.

6. Conclusions

Based on the geochronological, geochemical, and Sr–Nd–Hf isotopic studies presented here, we draw the following conclusions:

(1) U–Pb zircon dating results indicate that the dolerite dikes were intruded at 210.3 ± 1.5 Ma. These rocks all formed in a post-orogenic extensional setting.
(2) Most of the mafic rocks are characterized by low $K_2O + Na_2O$, and belong to intergradational series (alkaline and calc-alkaline) in the TAS diagram. In addition, the mafic dikes are characterized by light REE (LREE) enrichment and heavy REE (HREE) depletion [$(La/Yb)_N = (4.9–5.8)$]; no Eu negative anomaly ($Eu/Eu^* = 1.01–1.17$); high Nb, Y, Sr, Ba, and Sc; and low Rb, Zr, Hf, U, Th, and Pb.
(3) The mafic dikes were derived through partial melting of an enriched mantle source itself related to lithospheric delamination. The parental magmas experienced fractional crystallization of olivine, clinopyroxene, hornblende, Ti-bearing phases, apatite, and zircon. Minor, unimportant, crustal contamination likely also occurred during magma ascent.

Acknowledgements

This research was supported by the National Nature Science Foundation of China (40673029 and 40773020). We are grateful to Dr Lian Zhou and Jinhui Yang for their help with the Sr, Nd, and zircon Hf isotopic analysis, and we thank Yong-sheng Liu and Zhao-Chu Hu for their help with LA–ICP–MS zircon U–Pb dating. The authors also thank Hu-jun Gong for helping with cathodoluminescence image handling.

References

Andersen, T., 2002, Correction of common lead in U–Pb analyses that do not report 204Pb: Chemical Geology, v. 192, p. 59–79.

Blichert-Toft, J., and Albare'de, F., 1997, The Lu–Hf geochemistry of chondrites and the evolution of the mantle–crust system: Earth and Planetary Science Letters, v. 148, p. 243–258.

Feng, G., Liu, S., Zhong, H., Feng, C., Coulson, I.M., Qi, Y., Yang, Y., and Yang, C., 2011, U–Pb zircon geochronology, geochemical, and Sr–Nd isotopic constraints on the age and origin of basaltic porphyries from western Liaoning Province, China: International Geology Review. doi: 10.1080/00206814.2011.605837.

Gao, S., Luo, T.-C., Zhang, B.-R., Zhang, H.-F., Han, Y.-W., Zhao, Z.-D., and Hu, Y.-K., 1998a, Chemical composition of the continental crust as revealed by studies in East China: Geochimica et Cosmochimica Acta, v. 62, p. 1959–1975.

Gao, S., Zhang, B.-R., Jin, Z.-M., Kern, H., Luo, T.-C., and Zhao, Z.-D., 1998b, How mafic is the lower continental crust?: Earth and Planetary Science Letters, v. 106, p. 101–117.

Goolaerts, A., Mattielli, N., de Jong, J., Weis, D., and Scoates, J.S., 2004, Hf and Lu isotopic reference values for the zircon standard 91500 by MC-ICP-MS: Chemical Geology, v. 206, p. 1–9.

Griffin, W.L., Pearson, N.J., Belousova, E., Jackson, S.E., van Achterbergh, E., O'Reilly, S.Y., and Shee, S.R., 2000, The Hf isotope composition of cratonic mantle: LAM-MC-ICPMS analysis of zircon megacrysts in kimberlites: Geochimica et Cosmochimica Acta, v. 4, p. 133–147.

Guo, C.L., Wu, F.Y., Yang, J.H., Lin, J.Q., and Sun, D.Y., 2004a, The extensional setting of the Early Cretaceous magmatism in eastern China: Example from the Yinmawanshan pluton in southern Liaodong Peninsula: Acta Petrologica Sinica, v. 20, p. 1193–1204.

Guo, F., Fan, W.M., Wang, Y.J., and Zhang, M., 2004b, Origin of early Cretaceous calc-alkaline lamprophyres from the Sulu orogen in eastern China: Implications for enrichment processes beneath continental collisional belt: Lithos, v. 78, p. 291–305.

Hall, H.C., 1982, The importance and potential of mafic dyke swarms in studies of geodynamic process: Geosciences Canada, v. 9, p. 145–154.

Hall, H.C., and Fahrig, W.F., 1987, Mafic dyke swarms: Geological Association of Canada Special Paper 34, p. 1–503.

HBGMR (Heilongjiang Bureau of Geology and Mineral Resources), 1993, Regional geology of Heilongjiang Province: Beijing, Geological Publishing House, p. 347–438 (in Chinese with English summary).

Hirajima, T., Ishiwatari, A., Cong, B., Zhang, R., Banno, S., and Nozaka, T., 1990, Coesite from Mengzhong eclogite at Donghai county, northern Jiangsu province, China: Mineralogy Magazine, v. 54, p. 579–583.

IMBGMR (Inner Mongolian Bureau of Geology and Mineral Resources), 1990, Regional geology of Inner Mongolian Autonomous Region: Beijing, Geological Publishing House, 725 p (in Chinese with English summary).

Jahn, B.M., Wu, F.Y., Lo, C.H., and Tsai, C.H., 1999, Crustmantle interaction induced by deep subduction of the continental crust: Geochemical and Sr–Nd isotopic evidence from post-collisional mafic–ultramafic intrusions of the northern Dabie complex, central China: Chemical Geology, v. 157, p. 119–146.

JBGMR (Jilin Bureau of Geology and Mineral Resources), 1988, Regional geology of Jilin Province: Beijing, Geological Publishing House, p. 301–385 (in Chinese with English summary).

Kato, T., Enami, A., and Zhai, M., 1997, Ultrahigh-pressure marble and eclogite in the Su–Lu ultrahigh-pressure terrane, eastern China: Journal of Metamorphic Geology, v. 15, p. 169–182.

Le Maitre, R.W., 2002, Igneous rocks: A classification and glossary of terms (2nd edition): Cambridge, Cambridge University Press, 236 p.

Liu, S., Hu, R.Z., Feng, G.Y., Yang, Y.H., Qi, Y.Q., and Wang, T., 2010a, The distribution and significance of the mafic dykes since Mesozoic in North China Craton: Geological Bulletin of China, v. 29, p. 259–267.

Liu, S., Hu, R., Gao, S., Feng, C., Feng, G., Coulson, I.M., Li, C., Wang, T., and Qi, Y., 2010b, Zircon U–Pb age and Sr–Nd–Hf isotope geochemistry of Permian granodiorite and associated gabbro in the Songliao Block, NE China and implications for growth of juvenile crust: Lithos, v. 114, p. 423–436.

Liu, S., Hu, R., Gao, S., Feng, C., Qi, Y., Wang, T., Feng, G., and Coulson, I.M., 2008a, U–Pb zircon age, geochemical and Sr–Nd–Pb–Hf isotopic constraints on age and origin of alkaline intrusions and associated mafic dikes from Sulu orogenic belt, Eastern China: Lithos, v. 106, p. 365–379.

Liu, S., Hu, R.-Z., Gao, S., Feng, C.-X., Qi, L., Zhong, H., Xiao, T., Qi, Y.-Q., Wang, T., and Coulson, I.M., 2008b, Zircon U–Pb geochronology and major, trace elemental and Sr–Nd–Pb isotopic geochemistry of mafic dykes in western Shandong Province, east China: Constrains on their petrogenesis and geodynamic significance: Chemical Geology, v. 255, p. 329–345.

Liu, S., Hu, R., Gao, S., Feng, C., Yu, B., Feng, G., Qi, Y., Wang, T., and Coulson, I.M., 2009, Petrogenesis of Late Mesozoic mafic dykes in the Jiaodong Peninsula, eastern North China Craton and implications for the foundering of lower crust: Lithos, v. 113, p. 621–639.

Liu, S., Hu, R.Z., Zhao, J.H., and Feng, C.X., 2004, K–Ar geochronology of Mesozoic mafic dikes in Shandong Province, Eastern China: Implications for crustal extension: Acta Geologica Sinica, v. 78, p. 1207–1213.

Liu, S., Su, W., Hu, R., Feng, C., Gao, S., Coulson, I.M., Wang, T., Feng, G., Tao, Y., and Xia, Y., 2010c, Geochronological and geochemical constraints on the petrogenesis of alkaline ultramafic dykes from southwest Guizhou Province, SW China: Lithos, v. 114, p. 253–264.

Liu, S., Zou, H.B., Hu, R.Z., Zhao, J.H., and Feng, C.X., 2006, Mesozoic mafic dikes from the Shandong Peninsula, North China Craton: Petrogenesis and tectonic implications: Geochemical Journal, v. 40, p. 181–195.

Ludwig, K.R., 2003, ISOPLOT 3.0: A geochronological toolkit for Microsoft excels: Berkeley Geochronology Center, Special publication no. 4.

Lugmair, G.W., and Harti, K., 1978, Lunar initial 143Nd/144Nd: Differential evolution of the lunar crust and mantle: Earth Planetary Science Letters, v. 39, p. 349–357.

Middlemost, E.A.K., 1972, A simple classification of volcanic rocks: Bulletin of Volcanology, v. 36, p. 382–397.

Middlemost, E.A.K., 1994, Naming materials in the magma/igneous rock system: Earth-Science Reviews, v. 74, p. 193–227.

Pei, F.P., Xu, W.L., Yang, D.B., and Zhao, Q.G., 2005, Zircon SHRIMP U–Pb age and the geological significance of the gabbros in Tonghua, Jilin Province, China: Science in China, v. 35, p. 393–398.

Qi, L., Hu, J., and Grégoire, D.C., 2000, Determination of trace elements in granites by inductively coupled plasma mass spectrometry: Talanta, v. 51, p. 507–513.

Qin, K., 1995, Geological features of magmatic sulfide Cu–Ni deposit at the Hongqiling, Jilin Province: Jilin Geology, v. 3, p. 17–30 (in Chinese with English abstract).

Rapp, R.P., Shimizu, N., and Norman, M.D., 2003, Growth of early continental crust by partial melting of eclogite: Nature, v. 425, p. 605–609.

Soderlund, U., Patchett, P.J., Vervoort, J.D., and Isachsen, C.E., 2004, The 176Lu decay constant determined by Lu–Hf and U–Pb isotope systematics of Precambrian mafic intrusions: Earth and Planetary Science Letters, v. 219, p. 311–324.

Song, B., and Qiao, X.F., 2008, Ages of the zircon from basalt of the Erdaogou formation and diabase dyke warms in Northern Liaonign, and their significances: Earth Science Frontiers, v. 15, p. 250–262.

Steiger, R.H., and Jäger, E., 1977, Subcommission on geochronology; convention on the use of decay constants in geochronology and cosmochronology: Earth and Planetary Science Letters, v. 36, p. 359–362.

Sun, S.S., and McDonough, W.F., 1989, Chemical and isotopic systematics of oceanic basalts: Implications for mantle composition and processes, *in* Saunders, A.D., and Norry, M.J., eds., Magmatism in the ocean basins: London, Geological Society Special Publication, p. 313–345.

Tarney, J., and Weaver, B.L., 1987, Geochemistry and petrogenesis of early Proterozoic dyke swarms, *in* Halls, H.C., and Fahrig, W.C., eds., Mafic dyke swarms, Volume 34: Geological Association of Canada Special Publication, p. 81–93.

Thompson, M., Potts, P.J., Kane, J.S., and Wilson, S., 2000, An international proficiency test for analytical geochemistry laboratories – Report on Round 5 (August 1999): Geostandards and Geoanalytical Research, v. 24, p. E1–E28.

Wang, X., Griffin, W.L., Wang, Z., and Zhou, X.M., 2003, Hf isotope compositions of zircons and implications for the petrogenesis of Yajiangqiao granite, Hunan Province, China: Chinese Science Bulletin, v. 48, p. 995–998.

Wilde, S.A., Zhang, X.Z., and Wu, F.Y., 2000, Extension of a newly identified 500 Ma metamorphic terrane in North East China: Further U–Pb SHRIMP dating of the Mashan Complex, Heilongjiang Province, China: Tectonophysics, v. 328, p. 115–130.

Wood, D.A., Tarneu, J., Varet, J., Saunders, A.N., Bouhault, H., Joron, J.L., Treuil, M., and Cann, J.R., 1979, Geochemistry of basalts drills in the North Atlantic by IPOD Leg 49: Implications for mantle heterogeneity: Earth and Planetary Science Letters, v. 42, p. 77–97.

Woodhead, J., Hergt, J., Shelley, M., Eggins, S., and Kemp, R., 2004, Zircon Hf-isotope analysis with an excimer laser, depth profiling, ablation of complex geometries, and concomitant age estimation: Chemical Geology, v. 209, p. 121–135.

Wu, F.Y., Jahn, B.M., Wilde, S.A., Lo, C.H., Yui, T.F., Lin, Q., Ge, W.C., and Sun, D.Y., 2003a, Highly fractionated I-type granites in NE China (I): Geochronology and petrogenesis: Lithos, v. 66, p. 241–273.

Wu, F.Y., Jahn, B.M., Wilde, S.A., Lo, C.H., Yui, T.F., Lin, Q., Ge, W.C., and Sun, D.Y., 2003b, Highly fractionated I-type granites in NE China (II): Isotopic geochemistry and implications for crustal growth in the Phanerozoic: Lithos, v. 67, p. 191–204.

Wu, F.Y., Sun, D.Y., Jahn, B.M., and Wilde, S.A., 2004, A Jurassic garnet-bearing granitic pluton from NE China showing tetrad REE patterns: Journal of Asian Earth Science, v. 23, p. 731–744.

Wu, F.Y., Sun, D.Y., Li, H.M., and Wang, X.L., 2001, The nature of basement beneath the Songliao Basin in NE China: Geochemical and isotopic constraints: Physics and Chemistry of the Earth (Part A), v. 26, p. 793–803.

Wu, F.Y., Yang, Y.H., Xie, L.W., Yang, J.H., and Xu, P., 2006, Hf isotopic compositions of the standard zircons and baddeleyites used in U–Pb geochronology: Chemical Geology, v. 234, p. 105–126.

Wu, F.Y., Ye, M., and Zhang, S.H., 1995, The geodynamic model of the Manzhouli–Suifenghe geoscience transect: Journal of Earth Science, v. 20, p. 535–539 (in Chinese with English abstract).

Xu, P., Wu, F.Y., Xie, L.W., and Yang, Y.H., 2004, Hf isotopic compositions of the standard zircons for U–Pb dating: Chinese Science Bulletin, v. 49, p. 1642–1648.

Yang, J., Godard, G., Kienast, J.R., Lu, Y., and Sun, J., 1993, Ultrahigh-pressure 60 kbar magnesite-bearing garnet peridotites from northeastern Jiangsu, China: Journal of Geology, v. 101, p. 541–554.

Yang, J.H., Wu, F.Y., Zhang, Y.B., Zhang, Q., and Wilde, S.A., 2004, Late Proterozoic zircons were found in Trias dolerites in northern Liaodong peninsula: Chinese Bulletin in Science, v. 49, p. 1878–1882.

Ye, M., Zhang, S.H., and Wu, F.Y., 1994, The classification of the Paleozoic tectonic units in the area crossed by Manzhouli–Suifenghe geoscience transect: Journal of Changchun University of Earth Sciences, v. 24, p. 241–245 (in Chinese with English abstract).

Yuan, H.L., Gao, S., Liu, X.M., Li, H.M., Gunther, D., and Wu, F.Y., 2004, Accurate U–Pb age and trace element determinations of zircon by laser ablation – inductively coupled plasma mass spectrometry: Geostandards Newsletter, v. 28, p. 353–370.

Zhang, H.F., Sun, M., Zhou, X.H., Fan, W.M., Zhai, M.G., and Yin, J.F., 2002, Mesozoic lithosphere destruction beneath the North China Craton: Evidence from major-, trace-element and Sr–Nd–Pb isotope studies of Fangcheng basalts: Contributions to Mineralogy and Petrology, v. 144, p. 241–253.

Zhang, H.F., Zhou, X.H., Fan, W.M., Sun, M., Guo, F., Ying, J.F., Tang, Y.J., Zhang, J., and Niu, L.F., 2005, Nature, composition, enrichment processes and its mechanism of the Mesozoic lithospheric mantle beneath the southeastern North China Craton: Acta Petrologica Sinica, v. 21, p. 1271–1280.

Zhang, R.Y., Liou, J.G., and Cong, B., 1994, Petrogenesis of garnet-bearing ultramafic rocks and associated eclogites in the Sulu ultrahigh-P metamorphic terrane, eastern China: Journal of Metamorphic Geology, v. 12, p. 169–186.

Zhao, J.X., and McCulloch, M.T., 1993, Melting of a subduction-modified continental lithospheric mantle: Evidence from late Proterozoic mafic dike swarms in central Australia: Geology, v. 21, p. 463–466.

Zhao, Q.Y., Li, C.F., Li, D.C., and Chen, Y.J., 2008, Dating for zircons fromgabbro dike of Wudaogou Group in Yanbian area and its geological significance: Global Geology, v. 27, p. 150–155 (in Chinese with English abstract).

Zhu, Z.P., Liu, L., Ma, R., Qiu, R.K., and Ma, S.H., 2009, 40Ar/39Ar isotopic dating and geological significance of mafic rocks from the Jixi Basin, Heilongjiang Province: Journal of Jilin University, v. 39, p. 238–243.